

Winter hydrometeorological extreme events modulated by large scale atmospheric circulation in southern Ontario

Olivier Champagne^{1*}, Martin Leduc², Paulin Coulibaly^{1,3}, M. Altaf Arain¹

¹ School of Geography and Earth Sciences, McMaster University, Hamilton, Ontario, Canada

² Ouranos and Centre ESCER, Université du Québec à Montréal, Montréal, Québec, Canada

³ Department of Civil Engineering, McMaster University, Hamilton, Ontario, Canada

Correspondence to: Olivier Champagne (champago@mcmaster.ca)

Abstract. Extreme events are widely studied across the world because of their major implications for many aspects of society and especially floods. These events are generally studied in term of precipitation or temperature extreme indices that are often not adapted for regions affected by floods caused by snowmelt. Rain on Snow index has been widely used but it neglects rain only events which are expected to be more frequent in the future. In this study, we identified a new winter compound index and assessed how large-scale atmospheric circulation controls the past and future evolution of these events in the Great Lakes region. The future evolution of this index was projected using temperature and precipitation from the Canadian Regional Climate Model Large Ensemble (CRCM5-LE). These climate data were used as input in PRMS hydrological model to simulate the future evolution of high flows in three watersheds in Southern Ontario. We also used five recurrent large-scale atmospheric circulation patterns in north-eastern North America and identified how they control the past and future variability of the newly created index and high flows. The results show that daily precipitation higher than 10mm and temperature higher than 5°C were necessary historical conditions to produce high flows in these three watersheds. In the historical period, the occurrences of these heavy rain and warm events as well as high flows were associated with two main patterns characterized by high Z500 anomalies centred on eastern Great Lakes (regime HP) and the Atlantic Ocean (regime South). These hydrometeorological extreme events will still be associated with the same atmospheric patterns in the near future. The future evolution of the index will be modulated by the internal variability of the climate system as higher Z500 in the east coast will amplify the increase in the number of events, especially the warm events. The relationship between the extreme weather index and high flows will be modified in the future as the snowpack reduces and rain becomes the main component of high flows generation. This study shows the values of CRCM5-LE dataset to simulate hydrometeorological extreme events in Eastern Canada and to better understand the uncertainties associated with internal variability of climate.

1 Introduction

According to the actual pathway of greenhouse gases emissions, temperature will continue to rise in the future with serious implications for society (Hoegh-Guldberg et al., 2018). The amount of precipitation, especially for extreme events, is also projected to increase globally (Kharin et al., 2013), due to the acceleration of the hydrological cycle (Trenberth, 1999). Because extreme precipitation has a great societal impact across the world, internationally coordinated climate indices, built from precipitation and temperature data, are widely used to assess the evolution of different weather extremes (Zhang et al., 2011). Some of these indices such as monthly or annual maximum of precipitation can be used to improve flood management. However, in catchments that receive snowfall, a large number of floods may occur due to a combination of temperature and precipitation extreme events such as Rain on Snow (ROS) (Merz and Blöschl, 2003). The impact of ROS on floods generation has been widely studied in different regions of the world, including Central Europe (Freudiger et al., 2014), the Alps (Würzer et al., 2016), the Rocky mountains (Musselman et al., 2018) or the New York State (Pradhanang et al., 2013). The projections of these events can be a challenge because they depend on the ability of the climate model to project the precipitation extremes and the aerial extent of snowmelt (McCabe et al., 2007). The climate models improvements allowed recent studies to project the future evolution of ROS (Jeong and Sushama, 2018; Musselman et al., 2018; Surfleet and Tullos, 2013). However strong uncertainties in the projections of such events remain, especially due to the internal variability of climate (Lafaysse et al., 2014). These uncertainties, even with the perfect climate model, will never be eradicated due to the inherently chaotic characteristic of the atmosphere (Lorenz, 1963; Deser et al., 2014). ROS are clearly controlled by large scale atmospheric circulation (Cohen et al., 2015) emphasizing the need to include internal climate variability uncertainties in the future evolution of ROS studies.

The Great Lakes region is one of the area of the world highly impacted by ROS events in winter (Buttle et al., 2016; Cohen et al., 2015). In this region, previous studies found correlations between precipitation (rain and snow) and temperature extremes and large-scale circulation indices: The negative phase of the Pacific North America oscillation (PNA⁻) brings more heavy precipitation events in the region south of the Great Lakes (Mallakpour and Villarini, 2016; Thiombiano et al., 2017) and more snowfall in the region North of the Great Lakes (Zhao et al., 2013), due to high moisture transport over the region (Mallakpour and Villarini, 2016). Another study showed a negative phase of PNA and positive phase of North Atlantic Oscillation (NAO) associated with warm days (Ning and Bradley, 2015). Temperature and precipitation uncertainties associated with climate internal variability have also been assessed in North America using a global climate model large ensemble (GCM-LE) (Deser et al., 2014). These studies generally separate precipitation and temperature while studying compound events, such as ROS,

has been recommended recently to improve our understanding of extreme impacts (Leonard et al., 2014). However, the definition of ROS index is also subjected to high uncertainties (Kudo et al., 2017) and this index may not be relevant in regions affected by significant rain only events (Jeong and Sushama, 2018). The goal of this study is to understand the impact of atmospheric circulation on winter hydrometeorological extreme events in the Great Lakes region. We will be using the Canadian Regional Climate Model Large Ensemble (CRCM5-LE), a 50-member regional model ensemble at a 12km resolution produced over north-eastern North America with the following objectives:

- (1) Define a regional precipitation and temperature compound index that explains the variability of winter high flows in Southern Ontario, which is the most populated area in the Great Lakes region.
- (2) Assess the relationship between this index and the recent large-scale atmospheric circulation.
- (3) Investigate the pertinence of the index to explain the future evolution of projected high flows and
- (4) Demonstrate how internal variability of climate will modulate the future evolution of atmospheric circulation and number of hydrometeorological extreme events in the region.

2 Data and methods

2.1 Climate data

Observations of precipitation, minimum temperature and maximum temperature for the winter months (DJF) in the 1957-2012 period were taken from NRCANmet produced by McKenney et al., (2011). These data were generated from an interpolation of Natural Resources Canada and Environment and Climate Change Canada data (ECCC) archives at 10 km spatial resolution. The simulated evolution of precipitation and temperature are from the Canadian Regional Climate Model Large Ensemble (CRCM5-LE). CRCM5-LE is a 50-member regional model ensemble at 12km resolution produced over north-eastern North America in the scope of the Québec-Bavaria international collaboration on climate change (ClimEx project; Leduc et al., 2019). CRCM5-LE is the downscaled version of the 310km resolution global Canadian model large ensemble (CanESM2-LE, Fyfe et al., 2017; Sigmond et al., 2018). The advantage of using a fine resolution large ensemble is that the processes at a local scale are better represented than a global ensemble and the local climate from each member of CRCM5-LE can be related to atmospheric circulation from CanESM2-LE. Temperature and precipitation from each member of CRCM5-LE have been bias corrected following the method of Ines and Hansen (2006) and using the observations and CRCM5-LE in the 1957-2012 period. For each month of the year, the intensity distribution of

temperature was corrected using a normal distribution. For the bias correction of precipitation, the frequency and the daily intensity were bias corrected separately: The precipitation frequency was first corrected by truncating the modelled frequency distribution in order to match the observed distribution. The truncated distribution of precipitation intensity was then corrected with a gamma distribution (Ines and Hansen, 2006). Each CRCM5-LE grid point has been bias-corrected in the 1957-2055 period using the closest NRCANmet point. Using a unique NRCANmet point for each CRCM5-LE point is permitted in our study because of low elevation gradients between points, the spatial variability of temperature and precipitation being more dependent on the proximity of the lakes than the elevation (Scott and Huff, 1996). The bias corrected CRCM5-LE data are reported at each NRCANmet point.

2.2 Heavy rain and warm index

Streamflow observations from three watersheds in southern Ontario (Figure 1) were used to define the daily temperature and precipitation thresholds needed to generate high flows in winter. A high flow event was defined for each watershed as streamflow higher than the 99th percentile. When more than two days in a row were selected, the events were considered as a single event and only the day with the highest high flow was considered. Figure 2 shows for each high flow event the distribution of daily temperature and precipitation amounts from all grids of the watersheds. Only events that produced high flows at least in 2 of the 3 watersheds are shown in Figure 2. The precipitation and temperature data are from the day situated three days before the high flow event for Big Creek watershed and two days before the high flow event for Thames and Grand rivers. This lag corresponds to the delay between a rainfall and/or warm event and the peak flow at the outlet. Figure 2 shows a maximum temperature higher than 5°C and precipitation higher than 10mm for most grid points during the high flow events. The index is therefore defined by the number of days with a temperature higher than 5°C and precipitation higher than 10mm. This index defines days with a significant rain and warm event that has the potential to generate a high flow event. The 5°C threshold gives a strong indication that precipitation is in a form of rain, and that the eventual snow in the ground is melting. This index is similar to the Rain on Snow index (ROS) defined by previous studies. The threshold of 10 mm was previously used to define ROS events with floods potential (Cohen et al., 2015; Musselman et al., 2018). Our newly created index can be defined rather as a heavy rain and warm index because snowpack is not integrated in the calculation.

2.3 Atmospheric circulation patterns

The recurrent atmospheric patterns in north-eastern North-America were identified by a weather regimes technique computed by a k-means algorithm (Michelangeli et al., 1995). The algorithm used daily geopotential height anomalies at 500hPa level (Z500) from the 20th century reanalyses (20thCR, Compo et al., 2011) and was applied in the 1957-2012 period to the north-eastern part of North America (30 N-60 N/110 W-50 W). Prior to the k-means calculations, we identified the principal components of the Z500 maps that explain 80% of the spatial variance. These principal components have been decomposed in weather regimes thanks to the k-means algorithm. k-means identifies classes centroids using an iteration method that minimizes intra-regime Euclidean distance and maximizes inter-regime Euclidean distance between the principal components of each day. The algorithm is repeated 100 times for each number of class between 2 and 10. The choice of the final class number is decided by a red noise test. This test consists in assessing the significance of the decomposition against weather regimes calculated from 100 randomly generated theoretical datasets that have the same statistical properties than the original dataset. The weather regimes have been previously calculated for the same domain and the red noise test showed five classes as the most robust choice (Champagne et al., 2019a).

The eigenvectors of the principal components calculated with 20thCR have been used to calculate the daily principal components for each member of CanESM2-LE. This transformation was applied to the daily Z500 normalized anomalies calculated for periods of 30 years between 1950 and 2099. By calculating the anomalies for periods of 30 years we minimized the low frequency variability. Therefore, the internal variability of climate through the 50-members can be fully investigated. Each day of the principal component dataset was then placed to the closest class centroid among the 5 classes previously identified using the historical 20thCR Z500 anomalies. This process was done for each member of CanESM2-LE.

2.4 Hydrological modelling

The future evolution of high flows in the three watersheds have been simulated using the Precipitation Runoff Modelling System (PRMS). PRMS is a semi distributed conceptual hydrological model widely used in snow dominated regions (Dressler et al., 2006; Liao and Zhuang, 2017; Mastin et al., 2011; Surfleet et al., 2012; Teng et al., 2017, 2018). PRMS computes the water flowing between hydrological reservoirs (plan canopy interception, snowpack, soil zone, subsurface) for each hydrological response unit (HRU). For a general description of PRMS the reader is referred to Markstrom et al. (2015). Champagne et al. (2019a) previously applied PRMS to these three watersheds and extensively described the parametrization process. PRMS has been calibrated in the 1989-2009 period using Precipitation, minimum temperature and maximum temperature from NRCANmet. The three

step trial-and-error calibration approach applied to each watershed showed satisfactory results (Champagne et al., 2019a). The streamflow was simulated for each member of the ensemble in the 1957-2055 period using CRCM5-LE bias corrected data described in the section 2.1.

To quantify the winter change in number of high flows due to a change in number of weather extreme events, the theoretical high flows frequency change due to the occurrence change in number of heavy rain and warm events (OCC) have been calculated. For each member of the ensemble, the simulated historical number of high flows events (99th percentile) associated with each weather regime has been multiplied by the change factor between number of rain and warm events in the historical period (1961-1990) and in the future period (2026-2055). The difference between this calculated number of high flows and the historical number of high flows corresponds to OCC. The total change in number of high flows simulated by PRMS (TOT) corresponding to each weather regimes is finally subtracted by OCC for each ensemble member to account for a change in number of high flows not due to a change in number of heavy rain and warm events (DIF).

3 Results

3.1 Weather regimes in north-eastern North America

Five weather regimes have been identified in north-eastern North America according to the red noise test and show distinct weather patterns (Figure 3). The weather regimes computed with 20thCR data show two clear opposite patterns characterized by positive (HP) and negative (LP) geopotential height anomalies on the Great Lakes. The regime South was characterized by positive Z500 anomalies in the Atlantic Ocean and negative anomalies in the north-west part of the domain and was associated with southerly winds. The regime North-West had low geopotential height on the Gulf of Saint-Lawrence together with winds from the northwest over the Great Lakes region. Finally, the regime North-East was associated with low geopotential height in the Atlantic Ocean but high geopotential height close to the Arctic that drove north-eastern winds over the Great Lakes. The weather regimes calculated with CanESM2-LE data, using the k-means centroids identified with 20thCR anomalies, have very similar patterns in the historical period (1961-1990) (Figure 3). CanESM2 50 members average Z500 anomalies were generally less strong than the 20thCR weather regimes and the anomalies were slightly shifted to the south. Over the Great Lakes, 20thCR and CanESM2-LE Z500 anomalies were similar for most of the regimes excepted for regime South showing higher Z500 anomalies with CanESM2-LE. In the 2026-2055 period the weather regimes show meteorological systems in similar locations, but the anomalies are clearly weaker (Figure 3).

3.2 Validation of heavy rain and warm index and high flows simulated by CRCM5-LE

The ability of the bias corrected CRCM5-LE data to recreate the number of heavy rain and warm events relative to the number of occurrences of each weather regime is assessed in this section. For the heavy precipitation events the observations show higher number of events during the occurrence of regime HP (10% of all HP days) compared to other regimes, especially in the southern parts of the region (13% of all HP days) (Figure 4). The regime South shows the second largest occurrence of heavy precipitation events (7% of all South days) while the regime North-West was associated with the least number of observed heavy precipitation events (2% of all North-West days). The number of precipitation events associated with a regime LP is spatially variable with a large number of events limited to the Lake Huron shoreline (12% of all LP days). The number of heavy precipitation events per winter was generally well recreated by the regional ensemble in the historical period (Figure 4). The regime South is the exception with much more events with the 50 members average (11% of all South days) compared to the observations (7% of all South days). In southern areas the simulations were also slightly overestimating the number of heavy precipitation events during regime North-West while underestimating during regime HP (Figure 4).

Figure 5 shows that the observed number of warm events (7.5% of all days) were overall more frequent than the number of heavy precipitation events (5% of all days, Figure 4). The number of warm events occurred more frequently in southern areas, particularly in the Niagara peninsula between Lake Erie and Lake Ontario, where 12-14% of all days were considered as warm days (Figure 5). The observed warm events occurred mostly during regime HP (23% of all HP days) while they were non-existent during regime LP (Figure 5). The number of warm events was similar between regimes North-West, North-East and South in a large part of the area. In the Niagara peninsula more events were occurring during a regime South (15% of all South days). The simulated number of warm events averaged for all members overestimated the observations and represented 11% of all days (Figure 5). This discrepancy was due to an overestimation during regimes North-West and South (Figure 5). Specifically, the number of events per occurrence of regime South for the 50 members average (19% of all South days) was twice the number of events calculated with the observations (9%).

The number of compound events, heavy rain and warm temperature was more frequent in the area close to Lake Erie in both observations and simulations if we consider all weather regimes together (Figure 6). The number of events was overestimated by the ensemble mean in the northern parts of the region. In this region, many grid points show all members of the ensemble overestimating the number of events. Close to Lake Erie the overestimation was lower and even non-existent in the Niagara peninsula. These compound index heavy rain and warm events were more frequent during a regime HP in both observations and simulations (4.5% of all HP days).

The simulations show a similar number of events during a regime South (4.5% of all South days) but the results largely overestimated the observations (1.5% of all Souths days). Finally, the occurrences of events were very low for LP and North-West (Figure 6).

The historical distribution of streamflow associated with heavy rain and warm events for the observed streamflow (OBS), streamflow simulated with NRCANmet (CTL) and streamflow simulated for all CRCM5-LE members (ENS) are depicted in Figure 7. The results show an observed streamflow frequently higher than the high flows threshold when the heavy rain and warm events occurred during a regime HP. The streamflow simulated with NRCANmet weather data (CTL) is underestimated but show a similar inter-regime variability with higher streamflow during HP heavy rain and warm events compared to events associated with other weather regimes. The 50 simulations from CRCM5-LE show a less strong variability between weather regimes but again higher streamflow when heavy rain and warm events correspond to regimes HP. High flows are also occurring for other weather regimes especially regime South (Figure 7).

3.3 Future evolution of hydrometeorological extreme events

The number of heavy precipitation events simulated by CRCM5-LE is expected to increase between 1961-1990 and 2026-2055, with a maximum increase between 1 and 2 events per winter expected close to the Georgian Bay (Figure 8). The increase in the number of events is mainly expected during the regime South but also for the regime LP near Lake Huron. The increased frequency of warm events is expected to be even higher reaching a total increase of about 10 events per winter close to Lake Erie. The highest increase is expected for HP and South regimes and at a lower rate for regimes North-East and North-West. The number of compound events is expected to increase by 1 or 2 events per winter with a maximal increase between Lake Erie and Huron. The increase in the number of heavy rain and warm events is expected to concern mainly the regime South and HP (Figure 8).

The contribution of the trend in heavy rain and warm events to the trend in number of high flows has been investigated (Figure 9). Taking all weather regimes events together, the total change in number of high flows simulated by PRMS (TOT) is expected to increase in the future. The theoretical high flows frequency change due to the occurrence change in number of heavy rain and warm events (OCC) is slightly lower than the increase in TOT for most of the weather regimes (DIF positive, Figure 9). Regime HP shows an opposite result with higher OCC compared to TOT on average (DIF negative, Figure 9).

The 50-members distribution change in rainfall and snowfall amounts corresponding to all compound events simulated by PRMS at each watershed outlet have been investigated (Figure 10). The amount of snowmelt and rainfall taken together is generally decreasing but a large difference between members was simulated. Many

members show an increase in amount of rain and snowmelt especially during regime LP. The change in amount of snowmelt follows a similar decreasing trend for most of the cases but an increase in snowmelt during LP extreme days is expected, especially in Grand River. The amount of rainfall is slightly increasing for most of the members especially for LP in Thames river and Big Creek river.

3.4 Relationship between change in occurrence of weather regimes and extreme events

Correlations between change in occurrence of weather regimes and change in number of Rain and Warm events between 1961-1990 and 2026-2055 for the 50 members have been calculated for each grid point (Figure 11). The magnitude of the correlations between occurrence of weather regimes and warm events is higher compared to correlations with heavy precipitation events. The results show significant positive correlations (95% confidence) between warm events and the change in occurrence of regime HP and negative correlations (95% confidence) between warm events and the change in occurrence of regime LP/North-east. For the precipitation events the results varied spatially with few areas showing positive correlations for regime South (Figure 11). The compound index shows positive correlations between the number of events and regime HP close to Lake Erie and negative correlations between the number of events and regime LP near Lake Huron.

Inter-member correlations between a combination of weather regimes frequency change and heavy Rain and warm events frequency change averaged over the entire region have also been investigated (Table 1). The goal is to identify the impact of a combination of two weather patterns on the hydrometeorological events. The weather regimes are a discretization of a continuous process and the combination of weather regimes aim to show the impact of weather regimes interactions on local climate. The combinations of weather regimes have been done by summing the change of occurrence from the two regimes of each combination. The correlation between change of any weather regimes combinations and change in number of heavy precipitation events are not significant. The correlations between change in number of warm events and change in occurrence of weather regimes is improved when regime South is calculated with regime HP and when regime LP is calculated with regime North-East compared to correlations with regimes HP or LP only (Table 1). Concerning the compound index, the number of heavy rain and warm events is positively correlated to a combination of regime South-HP (significant at 95% confidence interval) and negatively correlated to a combination of North-East-LP and North-East-LP (significant at 90% confidence interval).

The correlations with the change in number of high flows in each watershed have also been investigated (Table 2) and shows significance in the Big Creek and Grand River watersheds. In both watersheds, LP and a combination LP-North-West are negatively correlated to high flows while a combination North-West-South is positively

correlated to high flows. In Grand River the number of high flows is also negatively correlated to a combination of regime HP-LP.

The change of heavy precipitation, warm and compound events frequency in respect to change in occurrence of regimes South, HP, LP and North-East for each member of the ensemble is shown in Figure 12. The correspondence between change in number of heavy precipitations events and change in number of occurrences of weather regimes is not clear, confirming the low correlations in Figure 11 and Table 1. Regarding the warm events, the large increase in occurrence of regime HP-South or large decrease in regimes LP-North-East are generally associated with a large increase in number of warm events confirming the results from Figure 11 and Table 1. Concerning the compound index, a high increase of HP and South occurrences does not systematically lead to a large increase in number of events (Figure 12).

4 Discussion

4.1 Atmospheric circulation and extreme weather events

The extreme weather events investigated in this study were identified from data that have been bias corrected by an univariate method (Ines and Hansen, 2006) that can potentially increase the simulation bias for variables depending equally strongly on more than one climatic driver (Zscheischler et al., 2019). In our study, the number of warm events was clearly overestimated in a large area of the domain (Figure 5) but the bias corrected data satisfactory recreated the number of heavy precipitation and number of compound events (Figure 4 et 6). Despite remaining biases in the simulated data, the bias correction improved the results compared to analysis using raw data (Supplementary material Figure S1 and S2). This univariate bias correction method has been chosen in this study because was satisfactory used in previous works in the region (Champagne et al., 2019b; Wazneh et al., 2017). Future studies should consider using multivariate bias corrected methods to further improve the simulation of compound indices.

The occurrence of heavy rain and warm events calculated from bias corrected temperature and precipitation data are modulated by specific atmospheric patterns in winter which corroborates previous studies in the Great Lakes region. These studies found that heavy precipitation and flooding events are associated with high geopotential height anomalies in the east coast of North America similarly to regimes HP or South (Mallakpour and Villarini, 2016; Zhang and Villarini, 2019; Farnham et al., 2018). Our results found differences between observations and simulations with more heavy precipitation events during regime HP in the observations while the simulations with CRCM5-LE show more precipitation events during regime South (Figure 4). The overestimation in the number

of precipitation events for regime South can be associated with the difference in pattern between regimes calculated with 20thCR and CanESM2-LE (Figure 3). Regime South calculated with CanESM2-LE shows Z500 anomalies shifted to the west and likely a more meridional flux compared to the regime South from 20thCR. The weather regimes associated with heavy precipitations in the Mid-west defined by Zhang and Villarini (2019) show high pressure anomalies on the east and low pressure on the west sides of the Great lakes similarly to regime South calculated with CanESM2-LE. The regime South calculated with 20thCR shows negative Z500 anomalies with a northern position compared to CanESM2-LE and therefore a stronger zonal flux while the regime South calculated with CanESM2-LE has likely a more meridional flux driving humidity from the Gulf of Mexico (Figure 3). This pattern also brings warm temperature events even though the regime HP brings even more warm events in both the observations and the ensemble average (Figure 5). Regime HP has similarities with the positive phase of the NAO, previously associated with warm winter temperature in the Great Lakes region (Ning and Bradley, 2015). The other weather regimes bring generally fewer heavy precipitation or warm events apart from regime LP bringing heavy precipitation close to Lake Huron (Figure 4). LP is not associated with warm events (Figure 5) suggesting that these extreme precipitations are in form of snow and likely from lake effect snow. Suriano and Leathers (2017) show that low pressure anomalies north-east from Great lakes bring major lake effects snow in the eastern shores of Lake Huron due to less zonal wind and cold outbreaks from the Arctic. The regime LP shows low geopotential height anomalies right on the Great lakes and the associated north-west winds on the Lake Huron are likely to bring lake effect snowfall in this area.

4.2 Future evolution of rain and warm events

The future increase in winter heavy precipitation events in Southern Ontario was already described in Deng et al., (2016). Compound events such as Rain on Snow (ROS) events have also been investigated by Jeong and Sushama (2018). These authors defined ROS events as liquid precipitation and snow cover higher than 1mm and found no significant trend of ROS events in the Great Lakes region, in continuity to what was observed in the past (Wachowicz et al., 2019). These studies show that the Great Lakes region is located between a region of increase ROS events due to increase of rainfall in the north and a decrease in ROS events due to decrease of snowpack in southern regions. Increase of rainfall and decrease of snowpack are both expected to occur in Southern Ontario (Figure 10) and are likely to cancel each other in term of ROS events. Our heavy rain and warm index does not consider snowpack and is expecting to be more frequent in the future (Figure 8). The increase of heavy rain and warm events is likely driven by warmer temperature shown by the increase of the compound events and warm events both occurring at a higher extent close to Lake Erie (Figure 8). The increase in extreme precipitation events

is less significant than the increase in warm events and is occurring mostly in the Northern parts of the area (Figure 8).

The future evolution of ROS or heavy rain and warm events corresponding to different weather patterns have not been yet investigated in previous literature. It is interesting to note that the future increase in the number of heavy rain and warm events are expected to occur only for the regimes HP and South, the number of events remaining very low for the other regimes (Figure 8). This result suggests that the global increase of mean temperature and precipitation is not sufficient to reach the 10 mm and 5°C threshold for LP, North-West and North-East regimes. More precipitation events are expected during regime LP but the temperature stays too low to increase the numbers of heavy rain and warm events (Figure 8). Regime North-West and North-East show an increase of warm events but not an increase in precipitation events and therefore the number of rain and warm events is not expected to increase.

4.3 Change in frequency of heavy rain and warm events partially modulated by the occurrence of weather regimes

Despite clear association between regimes HP/South and occurrences of rain and warm events, the uncertainties linked to internal variability of climate are not fully apprehended by the frequency of weather regimes. Members of the ensemble associated with a simultaneous high increase of regime HP and South frequencies are generally associated with higher increase in rainfall and warm events (Table 1) but the association is less straightforward than suggested by the correlation values (Figure 12) probably due to poor association between precipitation extremes and occurrence of weather regimes (Table 1 and Figure 11). Similar change in occurrences of South-HP weather regimes can lead to variable change in number of heavy rain and warm events (Figure 12). This suggests that other scales than the weather regimes calculated in the northeastern North American domain are likely to play a role in weather extreme events and especially the change of heavy rain and warm events and precipitation events. The presence of the Great lakes has a large role in the variability of precipitation at a local scale (Martynov et al., 2012) suggesting that variability of precipitation events depend not so much on the atmospheric circulation over the Great Lakes at the day of the events. The temperature of the lakes and the amount of ice covering the lakes plays for example a great role in the variability of precipitation (Martynov et al., 2012).

4.4 Non stationarity in the relationship between weather extreme events and high flows

The projections show that the increase in number of high flows associated with a regime HP is expected to be lower than the increase in number of heavy rain and warm events (negative DIF in Figure 9). This result suggests

that the conditions to produce high flows may change in the future. As the temperature increase, snowmelt is expected to be a less important component in the generation of high flows in the region (Figure 10). In the historical period regimes HP and South produce approximately the same number of high flows in the simulations (Figure 7) but are driven mostly by heavy precipitation for the regime South and warm events for the regime HP (Figure 4 and 5). More importantly, HP shows a further increase of warm events in the future while South shows rather an increase of precipitation (Figure 8). In the context of less snow, the importance of precipitation to drive high flows will be higher in the future because warmer conditions do not increase snowmelt in case of a snowpack reduction (Figure 10). Therefore, the increase of weather extreme events associated with the regime South will generate an increase of high flows more strenuously than the increase of events associated with regime HP (Figure 9).

The future change in number of high flows is associated with a large inter-member uncertainty (Figure 9). The weather extreme events inter-member uncertainty was partly associated with the change in occurrence of weather regimes especially for the warm component (Figure 11,12 and Table 1). The association between occurrence of weather regimes and high flows is less clear and shows opposite results (Table 1 and 2). Especially, change of occurrence of regime North-West is positively correlated to the change in number of high flows in Big Creek and Grand river watersheds (Table 2) while it is negatively correlated to the change in number of weather extreme events in this area (Figure 11). The correlation is even significant when regimes North-west and South are associated (Table 2). This result can be due to the preferential sequence of weather regimes and more snow generated by patterns similar to the regime North-West (Champagne et al., 2019b). The pattern associated with regime North-west shows anticyclonic systems in the west part of the domain (Figure 3). The meteorological systems have a tendency to move eastward and this anticyclonic system is likely to become a regime South or HP (Champagne et al., 2019a, Supplementary material, Table S2). In addition, as already stated in the previous paragraph, regime HP will be less likely to produce a heavy rain event than a regime South in the future. Therefore, members projecting an increase in the combination of the snowy regime North-West and wetter and warmer regime South are more likely to project more high flow events. These results emphasize the need to study not only each hydrometeorological extreme events and relationship with atmospheric circulation independently, but also focusing on the sequence of weather patterns preceding the high flows events.

4.5 Relevance of rain and warm events to explain future evolution of high flows

The relevance of using an index based on daily temperature and precipitation to study the future evolution of high flows is questionable. Even if a heavy rain and warm event is a necessary condition to create a high flow event

(Figure 2), such event is not systematically followed by a high flow event (Figure 7). The previous section suggests that snow falling days before the high flow event has an important role in the generation of high flows. Other factors such as multi-days rain events could also contribute to increase the streamflow. This study focused on single day events to introduce first results in the ability of CRCM5-LE to recreate extreme events in southern Ontario, but future studies should investigate multi-day events.

Moreover, as stated in the previous section, the relationship between the extreme weather events index and high flows is affected by non-stationarity. Applied in the past, the Rain and warm index works well to define the high flows risk in Southern Ontario (Figure 2), the warm component of this index being a condition to trigger snowmelt. In a warming climate, snowpack is reduced, and the rain to snow ratio is increasing (Jeong and Sushama, 2018), changing the relationship between extreme weather events and high flows.

To integrate snow processes and reduce the uncertainties from non-stationarity of temperature, Rain on snow index could be used in lieu of our heavy rain and warm index. However, this index is not projected to be more frequent in the future in the Great Lakes region, precisely because of less snow in the ground (Jeong and Sushama, 2018). Moreover, ROS index integrates events with a very small contribution of snowmelt to the high flows while neglecting rainfall only events (Cohen et al., 2015; Jeong and Sushama, 2018; Pradhanang et al., 2013). The definition of ROS also introduces more uncertainties as it depends on the combination of simulated precipitation and temperature for several days (Kudo et al., 2017). Our heavy rain and warm index minimizes this uncertainty and take into consideration heavy rainfall whatever the amount of snow covering the ground. It is therefore a good tool to assess the potential risk of high flows in Southern Ontario from all ranges of rain events, even though it is important to keep in mind that the flood risk diminished as snowpack decreases. A rain only index could also be used but the impact of snowpack on streamflow would be completely eradicated while snow will still play a role in the future hydrology. ROS events, liquid precipitation events and our heavy rain and warm events, ideally with multi-day events integrated, should be investigated together to fully understand the future evolution of the flood risk due to a shift in weather extreme events.

5 Conclusion

The aim of this study was to assess the ability of the Canadian Regional Climate Model Large Ensemble (CRCM5-LE), a downscaled version of the 50-members global Canadian model Large Ensemble (CanESM2-LE), to simulate winter hydrometeorological extreme events in Southern Ontario and to investigate how the internal variability of climate will modulate the future evolution of these extremes. The winter composite index heavy rain

413 and warm temperature was identified in the past with gridded observation data (NRCANmet) by investigating
414 what conditions of temperature and precipitation are necessary to produce a high flow in three watersheds in
415 Southern Ontario. PRMS model was used to simulate the future evolution of high flows for each member of
416 CRCM5-LE in these three watersheds. The large-scale circulation patterns corresponding to these events were
417 assessed by identifying past recurrent weather regimes based on daily Z500 from the 20th century reanalyses and
418 estimating the evolution of the same weather regimes in the future for each member of CanESM2-LE. The results
419 of this study show that CRCM5-LE was able to:

420

421 (1) Recreate the historical larger number of events close to Lake Erie despite an overestimation of warm
422 events.

423 (2) Simulate more heavy rain and warm events as well as high flows during the regimes associated with high
424 pressure anomalies on the Great Lakes (HP) and the Atlantic-Ocean (South).

425 (3) Project an increase in the future number of heavy rain and warm events and associated high flows
426 especially during the regimes HP and South and in the vicinity of Lake Erie.

427

428 These results suggest that depending on the future evolution of natural variability of climate, the increase in the
429 number of events will be amplified or attenuated by the favoured positions of the pressure systems. The natural
430 variability of climate is not expected to greatly modulate the number of high flows due to an increase of the
431 importance of precipitation in generating high flows. The role of more localized processes such as impact of the
432 lakes on precipitation events needs to be further evaluated to improve the ability of the next versions of regional
433 climate models to recreate the precipitation events. The newly created weather index did not integrate snowpack
434 because the uncertainties in the ability of CRCM5-LE to recreate precipitation and temperature extremes at a daily
435 basis would be further increased in snowmelt estimates. However, snowpack variability will have a large impact
436 in the modulation of high flows in the region and future studies should investigate snow processes by taking
437 advantage of rapid improvements in climate regional modelling. Other regional climate models and different
438 scenarios should also be used to improve our understanding of the future evolution of hydrometeorological
439 extreme events in Southern Ontario. Despite these future possible improvements, our study gives a good
440 estimation of what to expect in term of change in number of hydrometeorological events in Southern Ontario and
441 will serve to better estimate the future flood risk in this populated region.

442 **Authors contribution**

443 ML furnished CRCM5-LE data. OC performed the analyses and made the figures. OC prepared the manuscript
444 with contributions from all co-authors.

445 **Competing interest**

446 The authors declare that they have no conflict of interest.

447 **Acknowledgement**

448 We are acknowledging the reviewers who gave constructive comments during the publication process. Financial
449 support for this study was provided by the Natural Sciences and Engineering Research Council (NSERC) of
450 Canada through the FloodNet Project. We also acknowledge support and contributions from Global Water Future
451 Program, Environment and Climate Change Canada, Natural Resources Canada and Water Survey of Canada.
452 The production of ClimEx was funded within the ClimEx project by the Bavarian State Ministry for the
453 Environment and Consumer Protection. The CRCM5 was developed by the ESCER centre of Université du
454 Québec à Montréal (UQAM; www.escer.uqam.ca) in collaboration with Environment and Climate Change
455 Canada. We acknowledge Environment and Climate Change Canada's Canadian Centre for Climate Modelling
456 and Analysis for executing and making available the CanESM2 Large Ensemble simulations used in this study,
457 and the Canadian Sea Ice and Snow Evolution Network for proposing the simulations. Computations with the
458 CRCM5 for the ClimEx project were made on the SuperMUC supercomputer at Leibniz Supercomputing Centre
459 (LRZ) of the Bavarian Academy of Sciences and Humanities. The operation of this supercomputer is funded via
460 the Gauss Centre for Supercomputing (GCS) by the German Federal Ministry of Education and Research and the
461 Bavarian State Ministry of Education, Science and the Arts.

462 **References**

463 Buttle, J. M., Allen, D. M., Caissie, D., Davison, B., Hayashi, M., Peters, D. L., Pomeroy, J. W., Simonovic, S.,
464 St-Hilaire, A. and Whitfield, P. H.: Flood processes in Canada: Regional and special aspects, Canadian Water
465 Resources Journal / Revue canadienne des ressources hydriques, 1–24, doi:10.1080/07011784.2015.1131629,
466 2016.

467 Champagne, O., Arain, M. A. and Coulibaly, P.: Atmospheric circulation amplifies shift of winter streamflow in
 468 Southern Ontario, *Journal of Hydrology*, 124051, doi:10.1016/j.jhydrol.2019.124051, 2019a.

469 Champagne, O., Arain, A., Leduc, M., Coulibaly, P. and McKenzie, S.: Future shift in winter streamflow
 470 modulated by internal variability of climate in southern Ontario, *Hydrology and Earth System Sciences*
 471 *Discussions*, 1–30, doi:10.5194/hess-2019-204, 2019b.

472 Cohen, J., Ye, H. and Jones, J.: Trends and variability in rain-on-snow events: RAIN-ON-SNOW, *Geophysical*
 473 *Research Letters*, 42(17), 7115–7122, doi:10.1002/2015GL065320, 2015.

474 Compo, G. P., Whitaker, J. S., Sardeshmukh, P. D., Matsui, N., Allan, R. J., Yin, X., Gleason, B. E., Vose, R. S.,
 475 Rutledge, G., Bessemoulin, P. and others: The twentieth century reanalysis project, *Quarterly Journal of the Royal*
 476 *Meteorological Society*, 137(654), 1–28, doi:10.1002/qj.776, 2011.

477 Deng, Z., Qiu, X., Liu, J., Madras, N., Wang, X. and Zhu, H.: Trend in frequency of extreme precipitation events
 478 over Ontario from ensembles of multiple GCMs, *Climate Dynamics*, 46(9–10), 2909–2921, doi:10.1007/s00382-
 479 015-2740-9, 2016.

480 Deser, C., Phillips, A. S., Alexander, M. A. and Smoliak, B. V.: Projecting North American climate over the next
 481 50 years: uncertainty due to internal variability*, *Journal of Climate*, 27(6), 2271–2296, 2014.

482 Dressler, K. A., Leavesley, G. H., Bales, R. C. and Fassnacht, S. R.: Evaluation of gridded snow water equivalent
 483 and satellite snow cover products for mountain basins in a hydrologic model, *Hydrological Processes*, 20(4), 673–
 484 688, doi:10.1002/hyp.6130, 2006.

485 Farnham, D. J., Doss-Gollin, J. and Lall, U.: Regional Extreme Precipitation Events: Robust Inference From
 486 Credibly Simulated GCM Variables, *Water Resources Research*, 54(6), 3809–3824,
 487 doi:10.1002/2017WR021318, 2018.

488 Freudiger, D., Kohn, I., Stahl, K. and Weiler, M.: Large-scale analysis of changing frequencies of rain-on-snow
 489 events with flood-generation potential, *Hydrology and Earth System Sciences*, 18(7), 2695–2709,
 490 doi:10.5194/hess-18-2695-2014, 2014.

491 Fyfe, J. C., Derksen, C., Mudryk, L., Flato, G. M., Santer, B. D., Swart, N. C., Molotch, N. P., Zhang, X., Wan,
 492 H., Arora, V. K., Scinocca, J. and Jiao, Y.: Large near-term projected snowpack loss over the western United
 493 States, *Nature Communications*, 8(1), doi:10.1038/ncomms14996, 2017.

494 Hoegh-Guldberg, O., Jacob, D., Taylor, M., Bindi, M., Brown, S., Camilloni, I., Diedhiou, A., Djalante, R., Ebi,
 495 K. L., Engelbrecht, F., Guiot, J., Hijioka, Y., Mehrotra, S., Seneviratne, S. I., Thomas, A., Warren, R., Halim, S.
 496 A., Achlatis, M., Alexander, L. V., Berry, P., Boyer, C., Byers, E., Brilli, L., Buckeridge, M., Cheung, W., Craig,
 497 M., Evans, J., Fischer, H., Fraedrich, K., Ganase, A., Gattuso, J. P., Bolaños, T. G., Hanasaki, N., Hayes, K.,
 498 Hirsch, A., Jones, C., Jung, T., Kanninen, M., Krinner, G., Lawrence, D., Ley, D., Liverman, D., Mahowald, N.,
 499 Meissner, K. J., Millar, R., Mintenbeck, K., Mix, A. C., Notz, D., Nurse, L., Okem, A., Olsson, L., Oppenheimer,
 500 M., Paz, S., Petersen, J., Petzold, J., Preuschmann, S., Rahman, M. F., Scheuffele, H., Schleussner, C.-F., Séférian,
 501 R., Sillmann, J., Singh, C., Slade, R., Stephenson, K., Stephenson, T., Tebboth, M., Tschakert, P., Vautard, R.,

502 Wehner, M., Weyer, N. M., Whyte, F., Yohe, G., Zhang, X., Zougmore, R. B., Marengo, J. A., Pereira, J. and
503 Sherstyukov, B.: Impacts of 1.5°C of Global Warming on Natural and Human Systems, , 138, 2018.

504 Ines, A. V. M. and Hansen, J. W.: Bias correction of daily GCM rainfall for crop simulation studies, *Agricultural
505 and Forest Meteorology*, 138(1–4), 44–53, doi:10.1016/j.agrformet.2006.03.009, 2006.

506 Jeong, D. and Sushama, L.: Rain-on-snow events over North America based on two Canadian regional climate
507 models, *Climate Dynamics*, 50(1–2), 303–316, doi:10.1007/s00382-017-3609-x, 2018.

508 Kharin, V. V., Zwiers, F. W., Zhang, X. and Wehner, M.: Changes in temperature and precipitation extremes in
509 the CMIP5 ensemble, *Climatic Change*, 119(2), 345–357, doi:10.1007/s10584-013-0705-8, 2013.

510 Kudo, R., Yoshida, T. and Masumoto, T.: Uncertainty analysis of impacts of climate change on snow processes:
511 Case study of interactions of GCM uncertainty and an impact model, *Journal of Hydrology*, 548, 196–207,
512 doi:10.1016/j.jhydrol.2017.03.007, 2017.

513 Lafaysse, M., Hingray, B., Mezghani, A., Gailhard, J. and Terray, L.: Internal variability and model uncertainty
514 components in future hydrometeorological projections: The Alpine Durance basin, *Water Resources Research*,
515 50(4), 3317–3341, doi:10.1002/2013WR014897, 2014.

516 Leduc, M., Mailhot, A., Frigon, A., Martel, J.-L., Ludwig, R., Brietzke, G. B., Giguère, M., Brissette, F., Turcotte,
517 R., Braun, M. and Scinocca, J.: The ClimEx Project: A 50-Member Ensemble of Climate Change Projections at
518 12-km Resolution over Europe and Northeastern North America with the Canadian Regional Climate Model
519 (CRCM5), *Journal of Applied Meteorology and Climatology*, 58(4), 663–693, doi:10.1175/JAMC-D-18-0021.1,
520 2019.

521 Leonard, M., Westra, S., Phatak, A., Lambert, M., van den Hurk, B., McInnes, K., Risbey, J., Schuster, S., Jakob,
522 D. and Stafford-Smith, M.: A compound event framework for understanding extreme impacts: A compound event
523 framework, *Wiley Interdisciplinary Reviews: Climate Change*, 5(1), 113–128, doi:10.1002/wcc.252, 2014.

524 Liao, C. and Zhuang, Q.: Quantifying the Role of Snowmelt in Stream Discharge in an Alaskan Watershed: An
525 Analysis Using a Spatially Distributed Surface Hydrology Model: ROLE OF SNOWMELT IN STREAMFLOW
526 IN ALASKA, *Journal of Geophysical Research: Earth Surface*, 122(11), 2183–2195, doi:10.1002/2017JF004214,
527 2017.

528 Lorenz, E. N.: Deterministic Nonperiodic Flow, *Journal of the Atmospheric Sciences*, 20(2), 130–141,
529 doi:10.1175/1520-0469(1963)020<0130:DNF>2.0.CO;2, 1963.

530 Mallakpour, I. and Villarini, G.: Investigating the relationship between the frequency of flooding over the central
531 United States and large-scale climate, *Advances in Water Resources*, 92, 159–171,
532 doi:10.1016/j.advwatres.2016.04.008, 2016.

533 Markstrom, S. L., Regan, R. S., Hay, L. E., Viger, R. J., Payn, R. A. and LaFontaine, J. H.: precipitation-runoff
534 modeling system, version 4: U.S. Geological Survey Techniques and Methods., 2015.

535 Martynov, A., Sushama, L., Laprise, R., Winger, K. and Dugas, B.: Interactive lakes in the Canadian Regional
536 Climate Model, version 5: the role of lakes in the regional climate of North America, *Tellus A: Dynamic*
537 *Meteorology and Oceanography*, 64(1), 16226, doi:10.3402/tellusa.v64i0.16226, 2012.

538 Mastin, M. C., Chase, K. J. and Dudley, R. W.: Changes in Spring Snowpack for Selected Basins in the United
539 States for Different Climate-Change Scenarios, *Earth Interactions*, 15(23), 1–18, doi:10.1175/2010EI368.1, 2011.

540 McCabe, G. J., Clark, M. P. and Hay, L. E.: Rain-on-Snow Events in the Western United States, *Bulletin of the*
541 *American Meteorological Society*, 88(3), 319–328, doi:10.1175/BAMS-88-3-319, 2007.

542 McKenney, D. W., Hutchinson, M. F., Papadopol, P., Lawrence, K., Pedlar, J., Campbell, K., Milewska, E.,
543 Hopkinson, R. F., Price, D. and Owen, T.: Customized Spatial Climate Models for North America, *Bulletin of the*
544 *American Meteorological Society*, 92(12), 1611–1622, doi:10.1175/2011BAMS3132.1, 2011.

545 Merz, R. and Blöschl, G.: A process typology of regional floods: PROCESS TYPOLOGY OF REGIONAL
546 FLOODS, *Water Resources Research*, 39(12), doi:10.1029/2002WR001952, 2003.

547 Michelangeli, P.-A., Vautard, R. and Legras, B.: Weather Regimes: Recurrence and Quasi Stationarity, *Journal*
548 *of the Atmospheric Sciences*, 52(8), 1237–1256, doi:10.1175/1520-0469(1995)052<1237:WRRAS>2.0.CO;2,
549 1995.

550 Musselman, K. N., Lehner, F., Ikeda, K., Clark, M. P., Prein, A. F., Liu, C., Barlage, M. and Rasmussen, R.:
551 Projected increases and shifts in rain-on-snow flood risk over western North America, *Nature Climate Change*,
552 8(9), 808–812, doi:10.1038/s41558-018-0236-4, 2018.

553 Ning, L. and Bradley, R. S.: Winter climate extremes over the northeastern United States and southeastern Canada
554 and teleconnections with large-scale modes of climate variability*, *Journal of Climate*, 28(6), 2475–2493, 2015.

555 Pradhanang, S. M., Frei, A., Zion, M., Schneiderman, E. M., Steenhuis, T. S. and Pierson, D.: Rain-on-snow
556 runoff events in New York: RAIN-ON-SNOW EVENTS IN NEW YORK, *Hydrological Processes*, 27(21), 3035–
557 3049, doi:10.1002/hyp.9864, 2013.

558 Scott, R. W. and Huff, F. A.: Impacts of the Great Lakes on regional climate conditions, *Journal of Great Lakes*
559 *Research*, 22(4), 845–863, 1996.

560 Sigmond, M., Fyfe, J. C. and Swart, N. C.: Ice-free Arctic projections under the Paris Agreement, *Nature Climate*
561 *Change*, 8(5), 404–408, doi:10.1038/s41558-018-0124-y, 2018.

562 Surfleet, C. G. and Tullos, D.: Variability in effect of climate change on rain-on-snow peak flow events in a
563 temperate climate, *Journal of Hydrology*, 479, 24–34, doi:10.1016/j.jhydrol.2012.11.021, 2013.

564 Surfleet, C. G., Tullos, D., Chang, H. and Jung, I.-W.: Selection of hydrologic modeling approaches for climate
565 change assessment: A comparison of model scale and structures, *Journal of Hydrology*, 464–465, 233–248,
566 doi:10.1016/j.jhydrol.2012.07.012, 2012.

567 Suriano, Z. J. and Leathers, D. J.: Synoptic climatology of lake-effect snowfall conditions in the eastern Great
568 Lakes region: SYNOPTIC CLIMATOLOGY OF LAKE-EFFECT SNOWFALL CONDITIONS, *International*
569 *Journal of Climatology*, 37(12), 4377–4389, doi:10.1002/joc.5093, 2017.

570 Teng, F., Huang, W., Cai, Y., Zheng, C. and Zou, S.: Application of Hydrological Model PRMS to Simulate Daily
571 Rainfall Runoff in Zamask-Yingluoxia Subbasin of the Heihe River Basin, *Water*, 9(10), 769,
572 doi:10.3390/w9100769, 2017.

573 Teng, F., Huang, W. and Ginis, I.: Hydrological modeling of storm runoff and snowmelt in Taunton River Basin
574 by applications of HEC-HMS and PRMS models, *Natural Hazards*, 91(1), 179–199, doi:10.1007/s11069-017-
575 3121-y, 2018.

576 Thiombiano, A. N., El Adlouni, S., St-Hilaire, A., Ouarda, T. B. M. J. and El-Jabi, N.: Nonstationary frequency
577 analysis of extreme daily precipitation amounts in Southeastern Canada using a peaks-over-threshold approach,
578 *Theoretical and Applied Climatology*, 129(1–2), 413–426, doi:10.1007/s00704-016-1789-7, 2017.

579 Trenberth, K. E.: Conceptual Framework for Changes of Extremes of the Hydrological Cycle with Climate
580 Change, *Climatic Change*, 42(1), 327–339, doi:10.1023/A:1005488920935, 1999.

581 Wachowicz, L. J., Mote, T. L. and Henderson, G. R.: A rain on snow climatology and temporal analysis for the
582 eastern United States, *Physical Geography*, 1–16, doi:10.1080/02723646.2019.1629796, 2019.

583 Wazneh, H., Arain, M. A. and Coulibaly, P.: Historical Spatial and Temporal Climate Trends in Southern Ontario,
584 Canada, *Journal of Applied Meteorology and Climatology*, 56(10), 2767–2787, doi:10.1175/JAMC-D-16-0290.1,
585 2017.

586 Würzer, S., Jonas, T., Wever, N. and Lehning, M.: Influence of Initial Snowpack Properties on Runoff Formation
587 during Rain-on-Snow Events, *Journal of Hydrometeorology*, 17(6), 1801–1815, doi:10.1175/JHM-D-15-0181.1,
588 2016.

589 Zhang, W. and Villarini, G.: On the weather types that shape the precipitation patterns across the U.S. Midwest,
590 *Climate Dynamics*, doi:10.1007/s00382-019-04783-4, 2019.

591 Zhang, X., Alexander, L., Hegerl, G. C., Jones, P., Tank, A. K., Peterson, T. C., Trewin, B. and Zwiers, F. W.:
592 Indices for monitoring changes in extremes based on daily temperature and precipitation data, *Wiley*
593 *Interdisciplinary Reviews: Climate Change*, 2(6), 851–870, doi:10.1002/wcc.147, 2011.

594 Zhao, H., Higuchi, K., Waller, J., Auld, H. and Mote, T.: The impacts of the PNA and NAO on annual maximum
595 snowpack over southern Canada during 1979-2009, *International Journal of Climatology*, 33(2), 388–395,
596 doi:10.1002/joc.3431, 2013.

597 Zscheischler, J., Fischer, E. M. and Lange, S.: The effect of univariate bias adjustment on multivariate hazard
598 estimates, *Earth System Dynamics*, 10(1), 31–43, doi:10.5194/esd-10-31-2019, 2019.

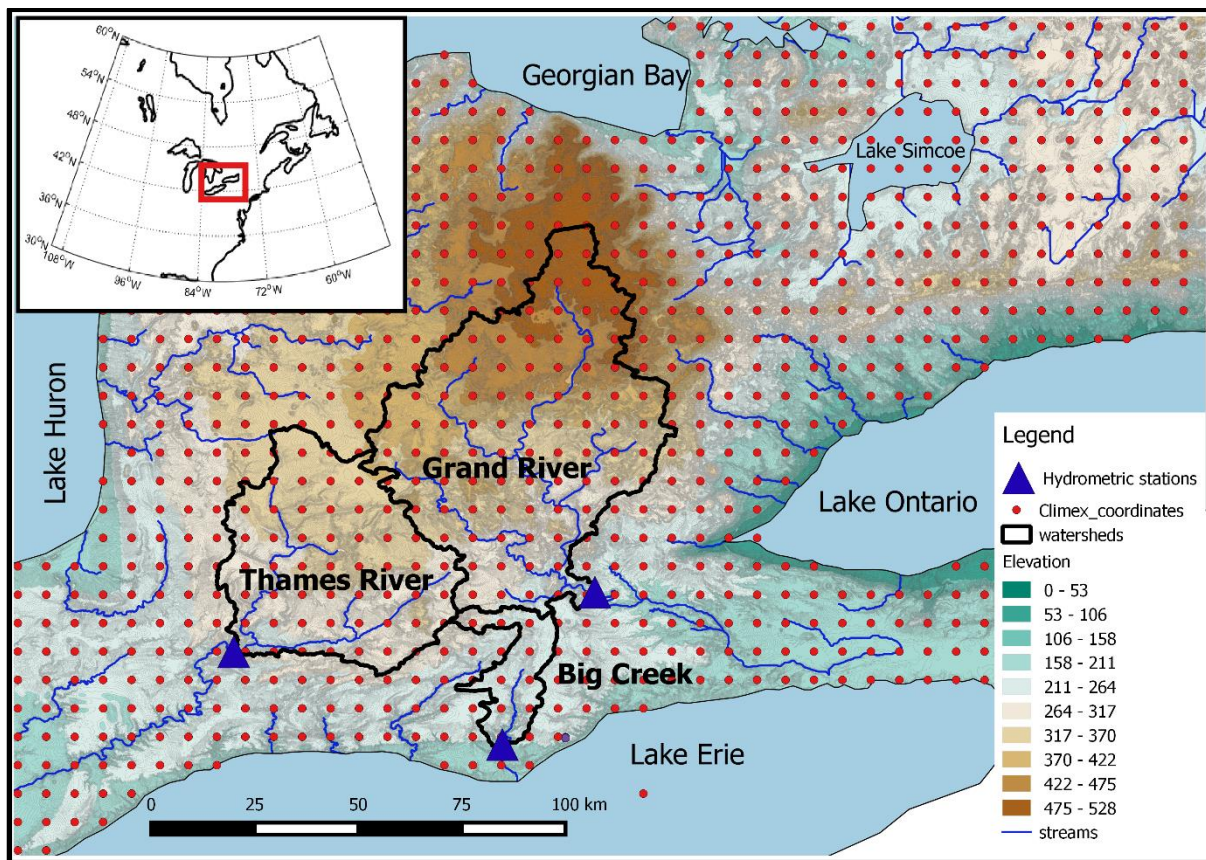


Figure 1: Location of the three watersheds and the ClimEx grid points used in this study and situation in the north-eastern North American domain (Inset). Elevation source: High Resolution Digital Elevation Model (HRDEM, Natural Resources Canada).

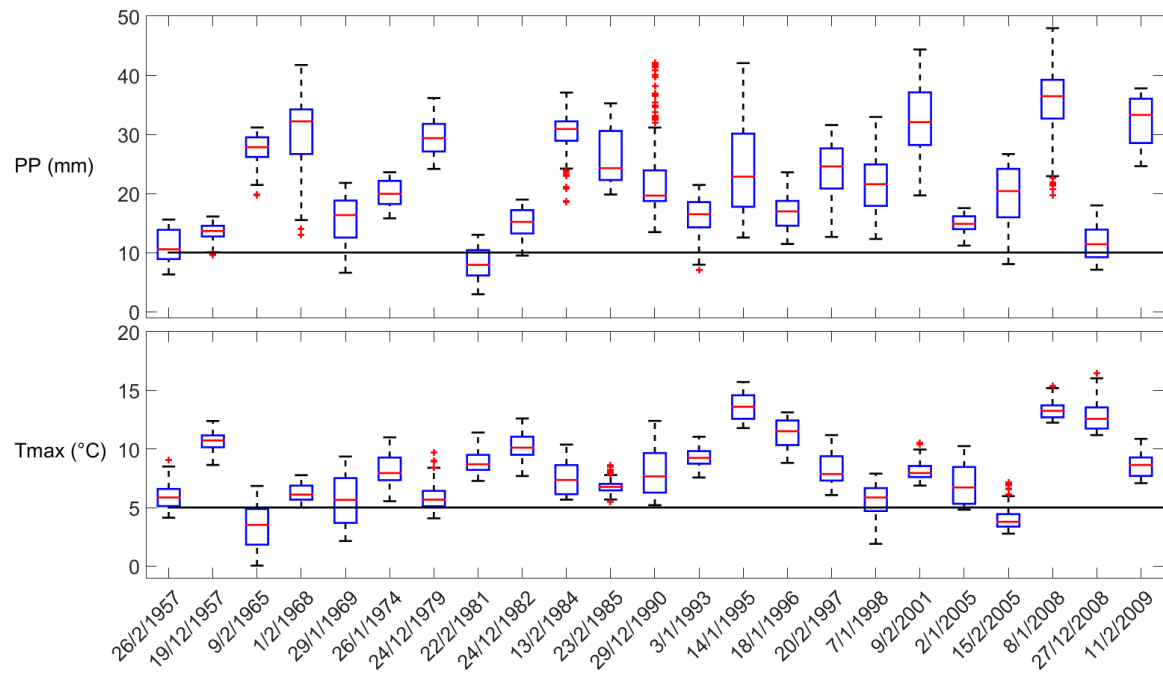
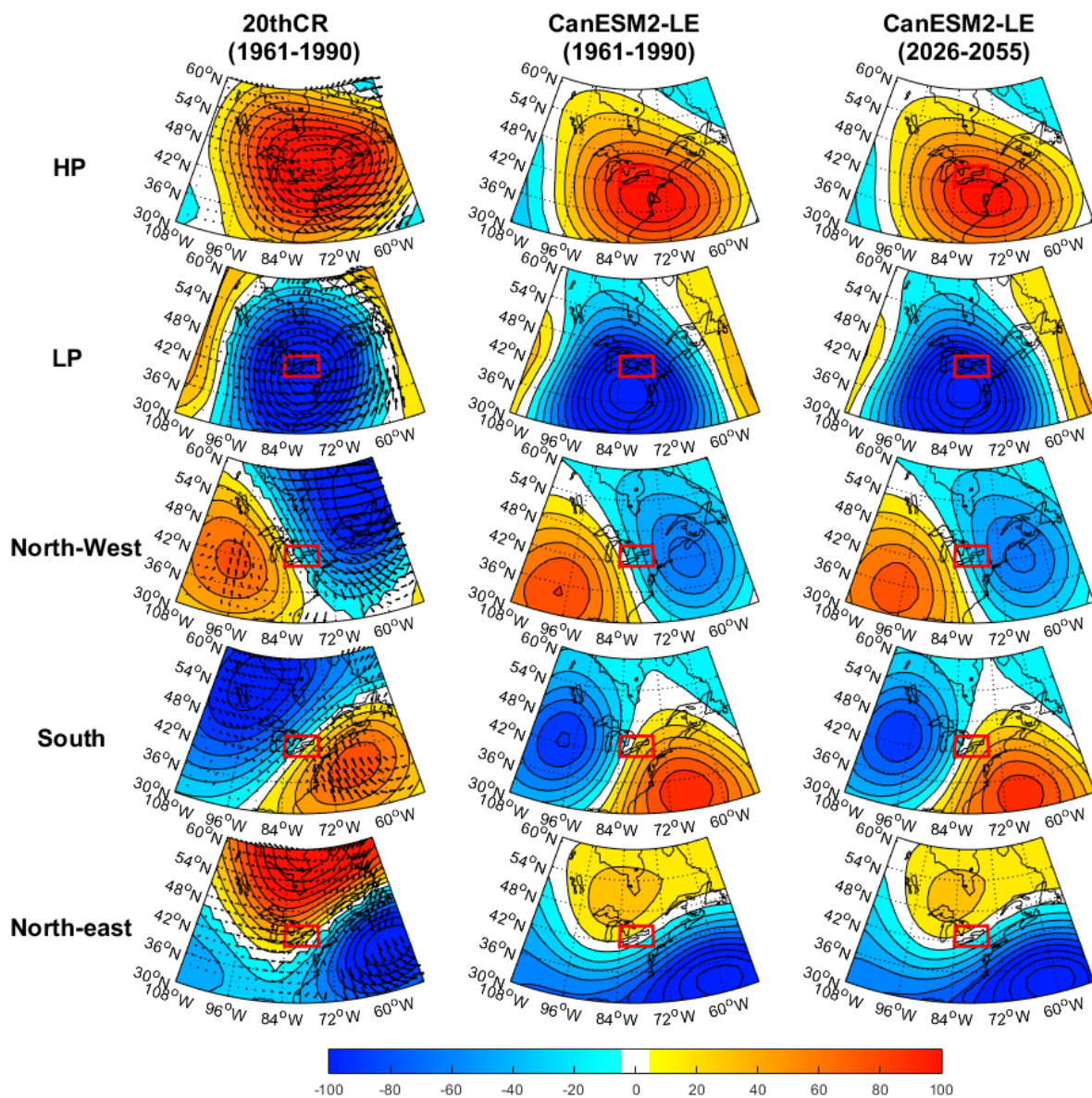


Figure 2: Distribution of NRCANmet temperature and precipitation from all 3 watersheds grid-points corresponding to each DJF high-flow event. Boxes extend from the 25th to the 75th percentile, with a horizontal red bar showing the median value. The whiskers are lines extending from each end of the box to the 1.5 interquartile range. Plus signs correspond to outliers. The horizontal black lines correspond to the thresholds used to define DJF weather extreme events.



609

610 Figure 3: Left panels: DJF Z500 anomalies (colours) and winds (vectors) corresponding to Weather Regimes calculated
 611 with 20thCR in the 1961-1990 period. Mid panels: DJF 50 members average Z500 anomalies calculated with CanESM2-
 612 LE in the 1961-1990 period. Right panels: DJF 50 members average Z500 anomalies calculated with CanESM2-LE in
 613 the 2026-2055 period.

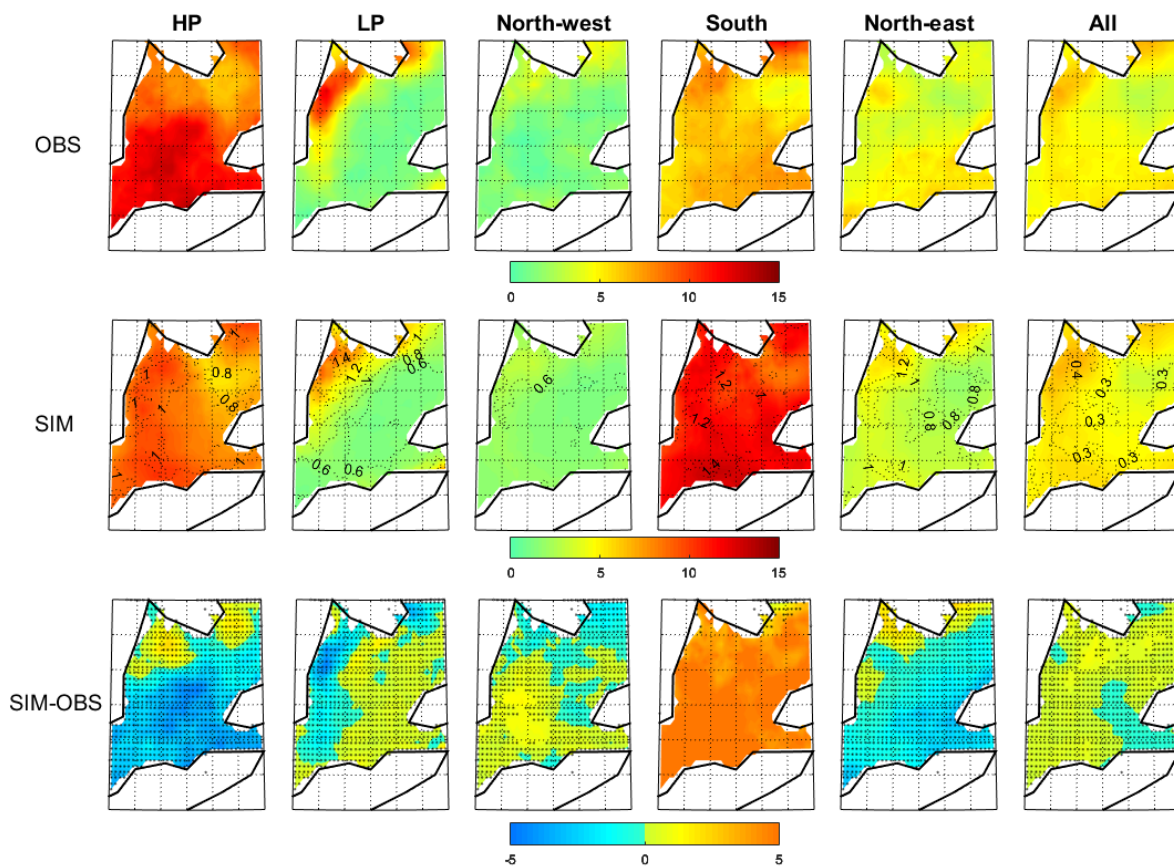


Figure 4: Percentage of DJF number of precipitation events ($P > 10\text{mm}$) relative to DJF occurrence of weather regimes in the historical period (1961-1990) for the observations (upper panels), simulations from CRCM5-LE 50 members average (mid panels) and simulations minus observations (lower panels). The dotted lines in the mid panels represent the standard deviation of the 50-members CRCM5-LE simulated percentage. Stippled regions in the lower panels indicate where the observations lie within the CRCM5-LE ensemble spread.

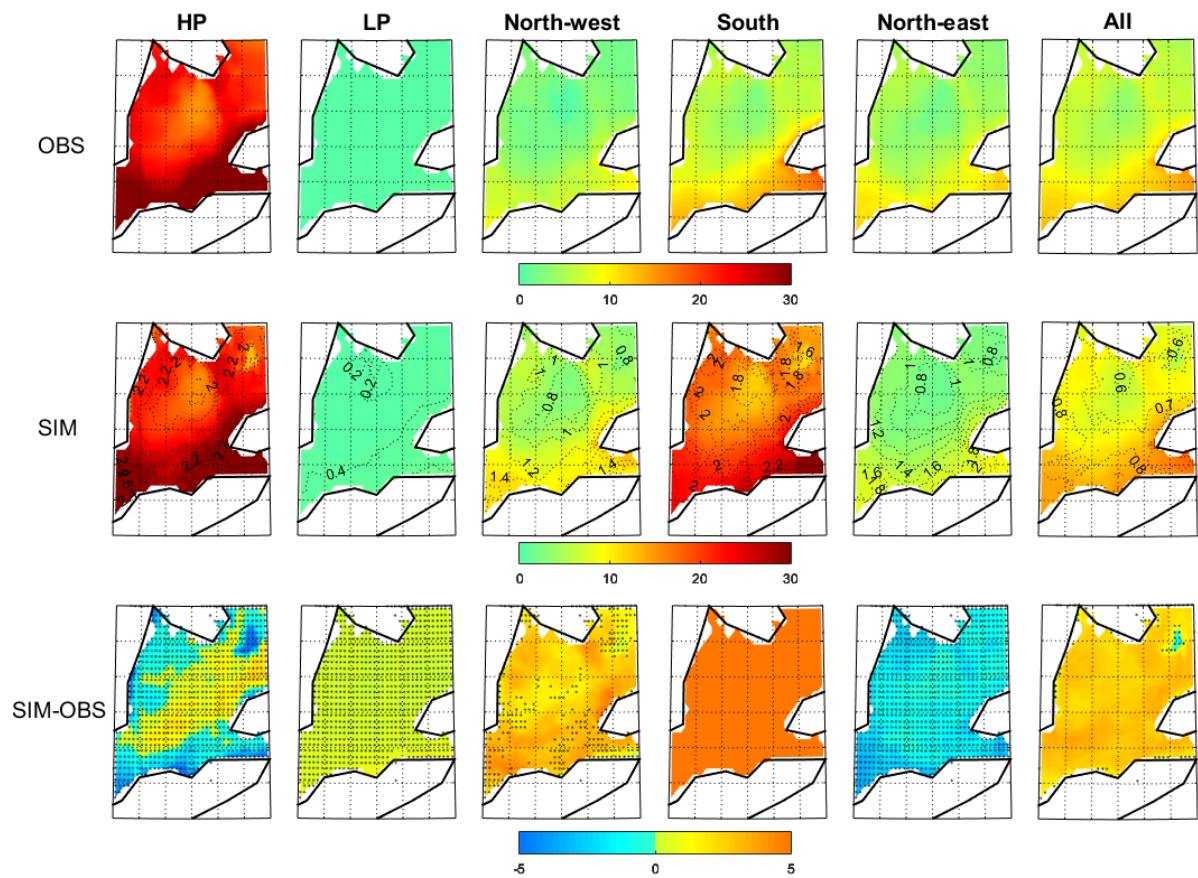


Figure 5: Percentage of DJF number of warm events ($T > 5^{\circ}\text{C}$) relative to DJF occurrence of weather regime in the historical period (1961-1990) for the observations (upper panels), simulations from CRCM5-LE 50 members average (mid panels) and simulations minus observations (lower panels). The dotted lines in the mid panels represent the standard deviation of the 50-members CRCM5-LE simulated percentage. Stippled regions in the lower panels indicate where the observations lie within the CRCM5-LE ensemble spread.

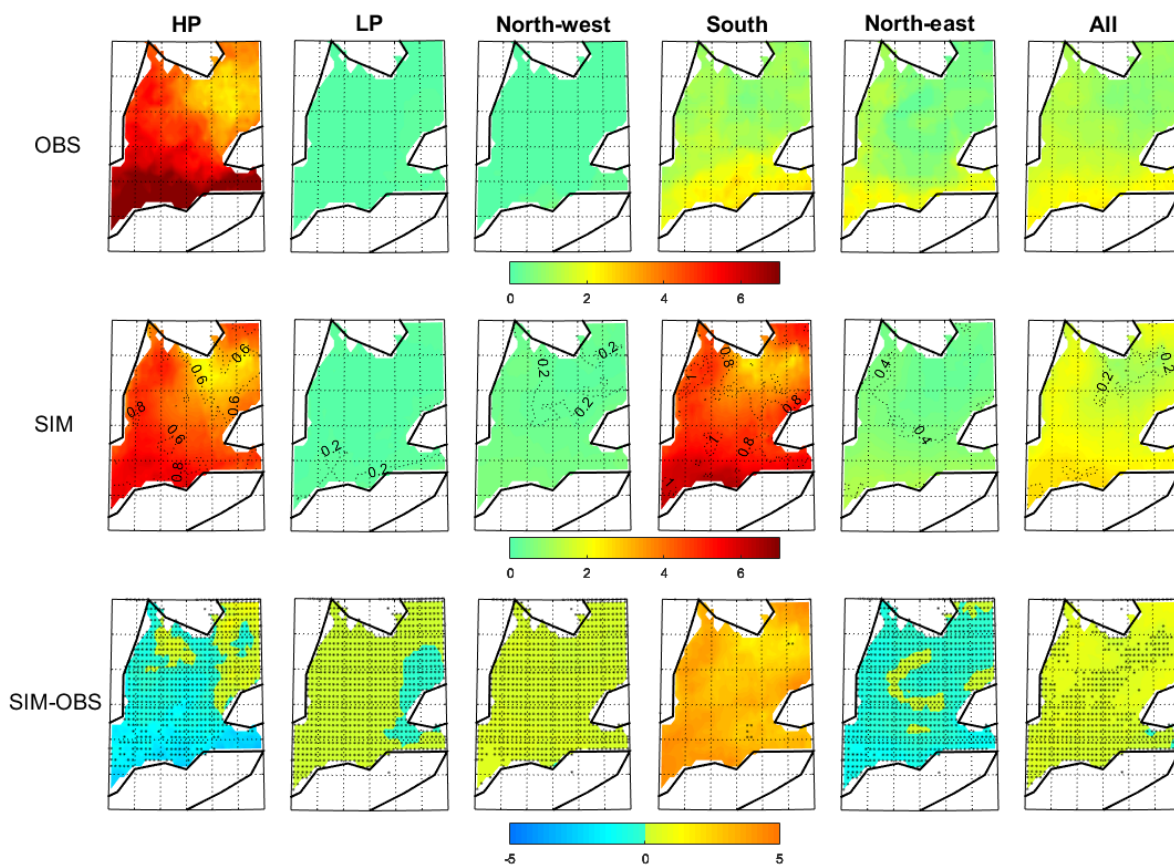


Figure 6: Percentage of DJF number of heavy rain and warm events ($P>10\text{mm}$ and $T>5^{\circ}\text{C}$) relative to DJF occurrence of weather regimes in the historical period (1961-1990) for the observations (upper panels), simulations from CRCM5-LE 50 members average (mid panels) and observations minus simulations (lower panels). The dotted lines in the mid panels represent the standard deviation of the 50-members CRCM5-LE simulated percentage. Stippled regions in the lower panels indicate where the observations lie within the CRCM5-LE ensemble spread.

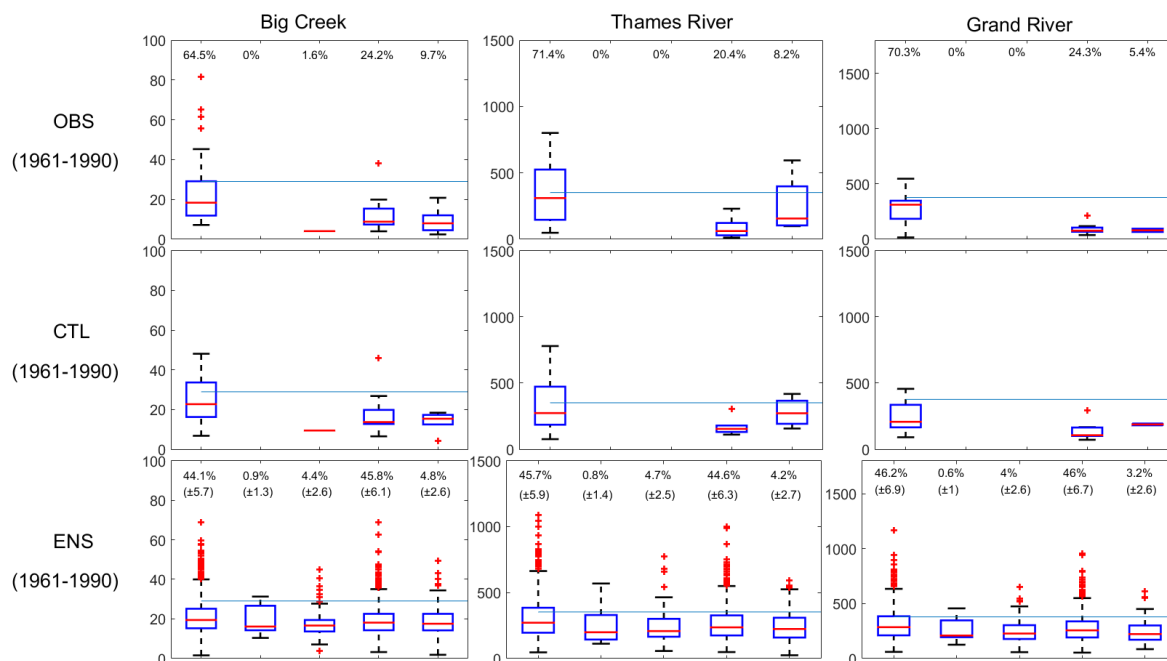


Figure 7: Upper and mid panels: Distribution of observed (OBS) and simulated (CTL) streamflow corresponding to all observed heavy rain and warm events. Lower panels: Distribution of simulated streamflow corresponding to all simulated heavy rain and warm events pooled for all members (ENS). Boxes extend from the 25th to the 75th percentile, with a horizontal red bar showing the median value. The whiskers are lines extending from each end of the box to the 1.5 interquartile range. Plus signs correspond to outliers. The horizontal blue lines correspond to high flows threshold (99th percentile).

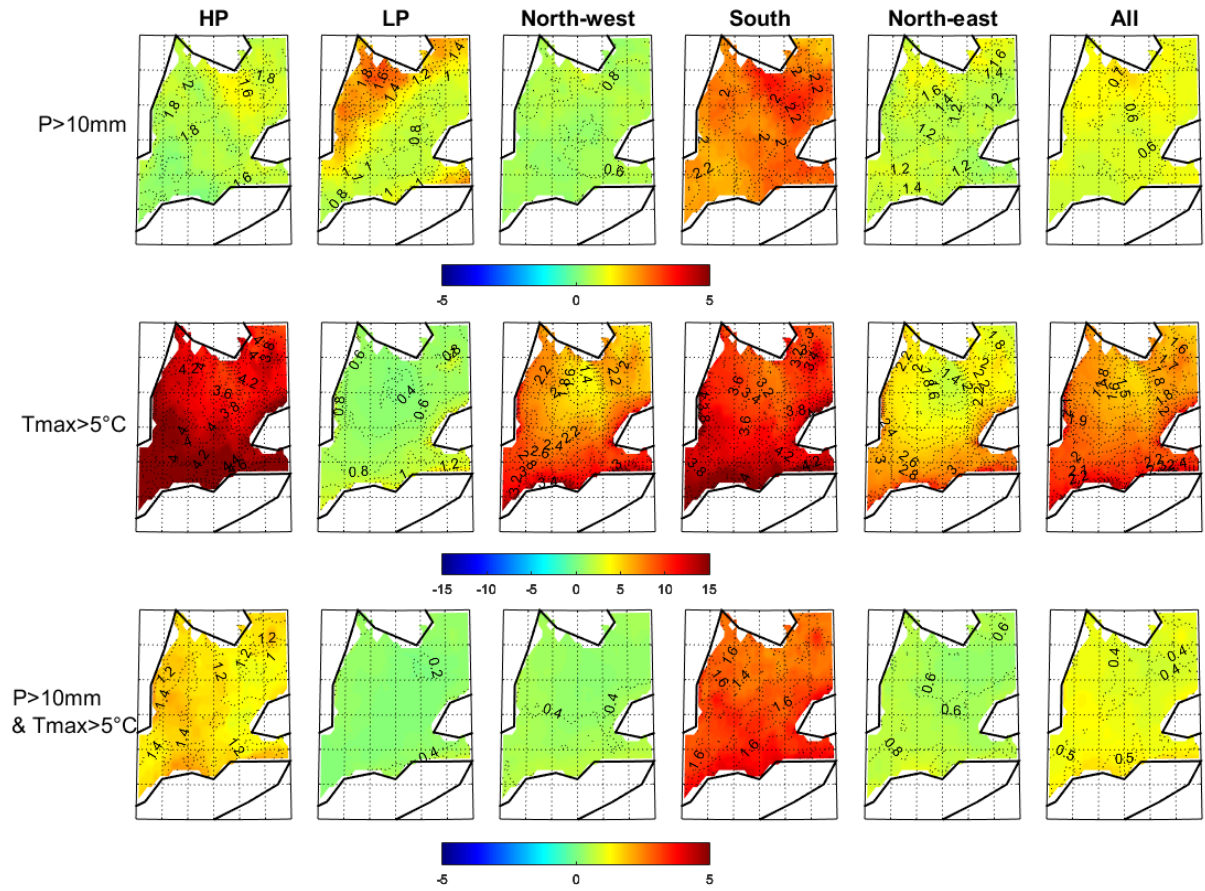


Figure 8: DJF change in CRCM5-LE average percentage of days with precipitation and warm events relative to DJF occurrence of weather regimes between the historical (1961-1990) and the future period (2026-2055). The dotted lines represent the standard deviation of the 50-members CRCM5-LE simulated change.

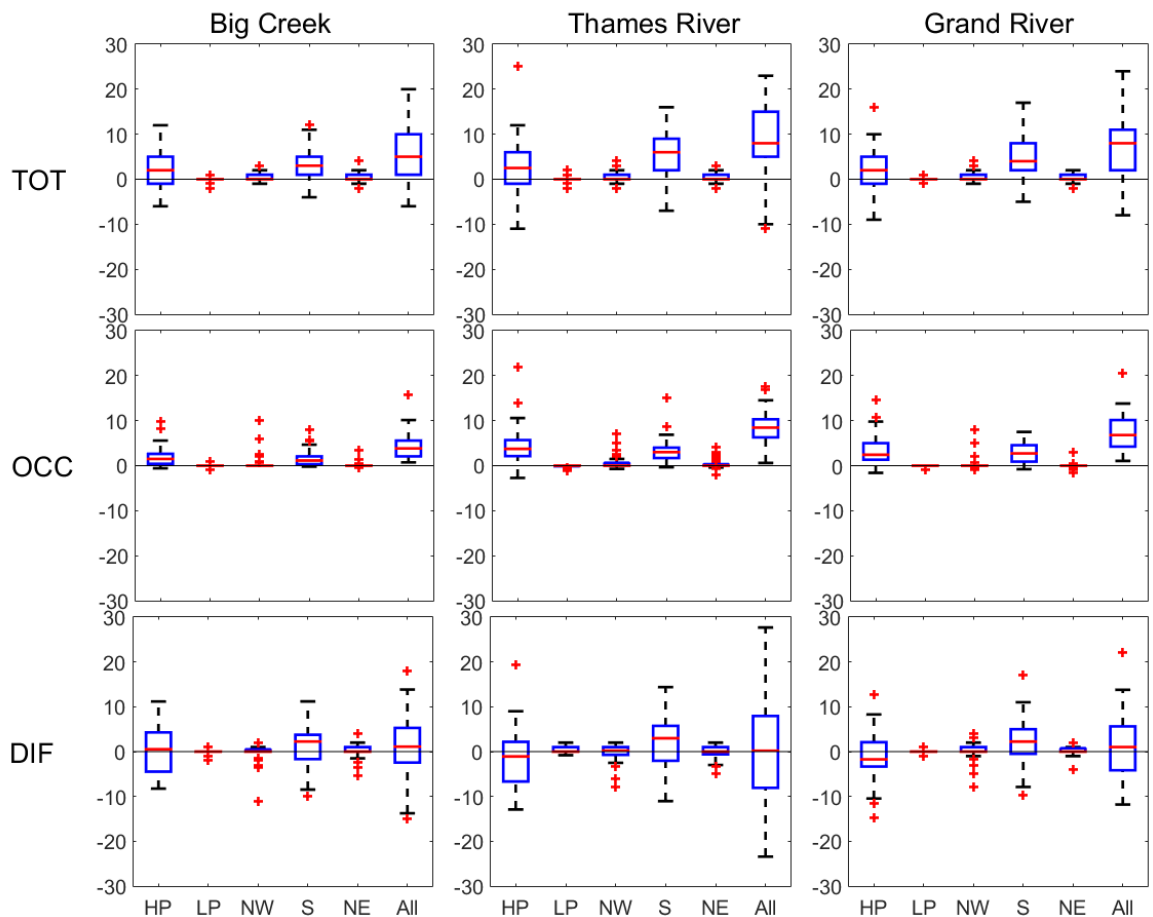


Figure 9: upper panels: Distribution of change in number of high flows between 1961-1990 and 2026-2055 simulated from the 50 members of the ensemble (TOT). Mid panels: Distribution of theoretical change in number of high flows using the factor of change in number of heavy rain and warm events between 1961-1990 and 2026-2055 (OCC). Lower panels: TOT minus OCC (DIF). Boxes extend from the 25th to the 75th percentile, with a horizontal red bar showing the median value. The whiskers are lines extending from each end of the box to the 1.5 interquartile range. Plus signs correspond to outliers.

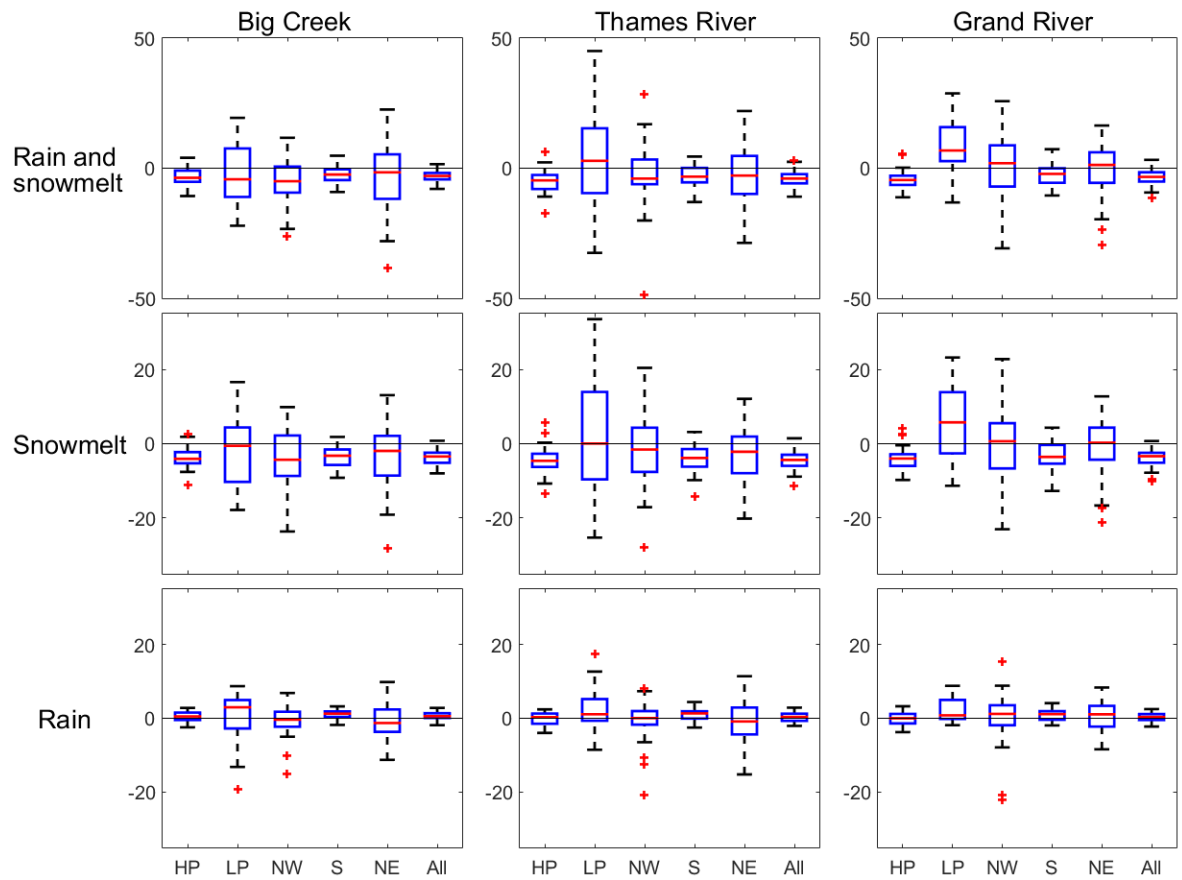


Figure 10: Distribution of simulated change in rain and snowmelt amounts (mm water equivalent) for all compound extreme events between 1961-1990 and 2026-2055 from the 50 members of the ensemble.

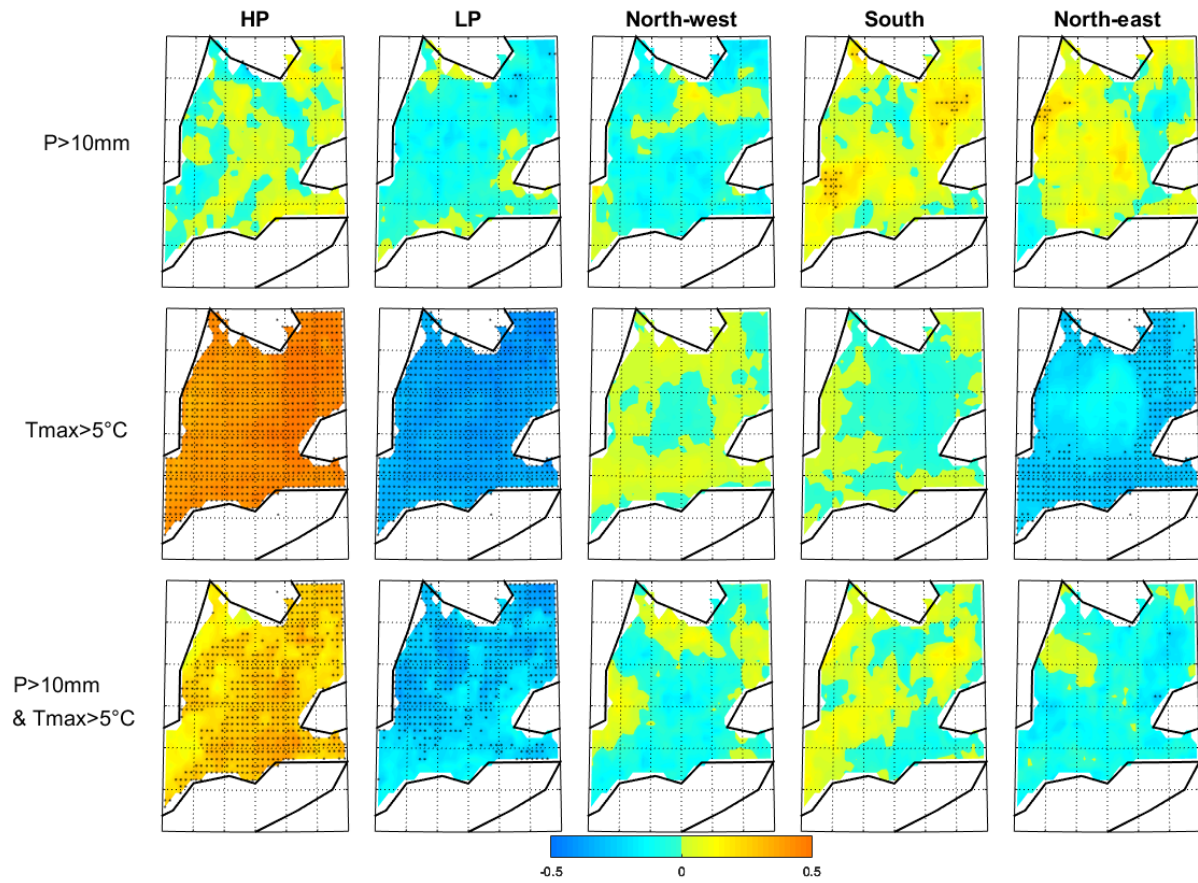


Figure 11: DJF inter-members correlations between change in occurrence of weather regimes and change in number of events between 1961-1990 and 2026-2055. Black points indicate a correlation significant at 95% according to the Pearson's correlation table.

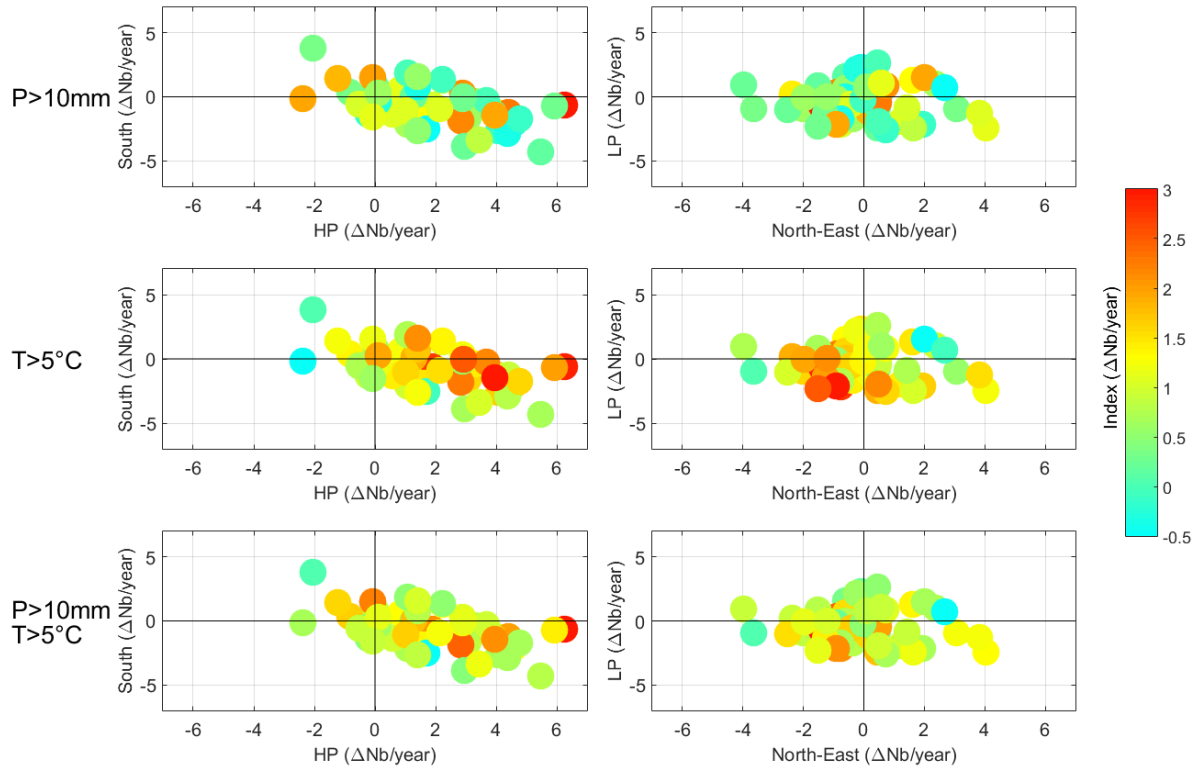


Figure 12: DJF change in occurrences of regimes HP-South (left) and LP-North-East (right) in respect to change in number of heavy rain and warm events (Colours) for each member of CRCM5-LE between 1961-1990 and 2026-2055.

670 Table 1: inter-members correlations between DJF change in occurrence of weather regimes and DJF change in number
671 of events between 1961-1990 and 2026-2055. Bold show correlations significant at 90% confidence level, a single
672 underline significant at 95% and double underline significant at 99% according to the Pearson's correlation table.

	P>10mm					Tmax>5°C					P>10mm & Tmax>5°C				
	HP	LP	NW	S	NE	HP	LP	NW	S	NE	HP	LP	NW	S	NE
HP	0.02	-0.04	-0.05	0.10	0.06	<u>0.45</u>	0.20	<u>0.38</u>	<u>0.48</u>	0.20	<u>0.30</u>	0.10	0.21	<u>0.35</u>	0.18
LP		-0.08	-0.14	0.02	-0.01		<u>-0.38</u>	-0.23	-0.25	<u>-0.45</u>		<u>-0.29</u>	-0.23	-0.17	-0.27
NW			-0.08	-0.01	-0.04			0.02	0.01	-0.20			-0.04	-0.02	-0.13
S				0.10	0.12				-0.01	-0.21				0.03	-0.06
NE					0.06					-0.25					-0.10

673
674 Table 2: inter-members correlations between DJF change in occurrence of weather regimes and DJF change in number
675 of high flows events between 1961-1990 and 2026-2055. Bold show correlations significant at 90% according to the
676 Pearson's correlation table.

	Big Creek					Thames River					Grand River				
	HP	LP	NW	S	NE	HP	LP	NW	S	NE	HP	LP	NW	S	NE
HP	0.00	-0.18	0.18	0.04	-0.08	0.06	-0.02	0.11	0.04	0.04	-0.05	-0.27	0.13	0.10	-0.10
LP		-0.24	0.05	-0.12	-0.25		-0.12	-0.02	-0.11	-0.10		-0.31	-0.01	-0.07	<u>-0.28</u>
NW			0.22	0.23	0.14			0.07	0.03	0.06			0.20	0.29	0.14
S				0.05	-0.05				-0.04	-0.05				0.18	0.06
NE					-0.11					-0.02					-0.09

677